Int. J. Heat Mass Transfer. Vol. 26, No. 8, pp. 1199–1205, 1983
Printed in Great Britain

0017-9310/83 $3.00 + 0.00
Pergamon Press Ltd.

CRITICAL HEAT FLUX ON A UNIFORMLY HEATED HORIZONTAL CYLINDER IN AN UPWARD CROSS FLOW OF SATURATED LIQUID

Y. KATTO and Y. HARAMURA
Department of Mechanical Engineering, University of Tokyo, Hongo, Bunkyo-ku, Tokyo, Japan

(*Received* 4 *September* 1982)

Abstract—This paper reports the results from an analytical study of the critical heat flux (CHF) on a uniformly heated horizontal cylinder in an upward cross flow of saturated liquid. Two kinds of vapor escape flow patterns are taken into account: one is the bubble-like flow in the range of very low velocities and the other is the sheet-like flow in the range of sufficiently high velocities. A new hydrodynamic instability model of CHF proposed recently by the authors is employed in the analysis, and it is shown that the prediction of CHF is fairly good when compared with the existing data.

NOMENCLATURE

A_v	cross-sectional area of vapor stems [m^2]
A_w	area of heated surface [m^2]
d	diameter of cylinder [m]
G	mass velocity of liquid, $u\rho_l$ [kg m^{-2} s^{-1}]
g	acceleration due to gravity [m s^{-2}]
H_{fg}	latent heat of evaporation [J kg^{-1}]
q	heat flux [W m^{-2}]
q_{c0}	critical heat flux in saturated boiling [W m^{-2}]
$q_{c0,Z}$	q_{c0} predicted by Zuber's equation (10) [W m^{-2}]
R'	dimensionless radius of cylinder, $(d/2)/[\sigma/g(\rho_l-\rho_v)]^{1/2}$
r	instantaneous radius of bubble [m]
s	instantaneous height of bubble center [m]
t	time [s]
u	velocity of bulk liquid flow [m s^{-1}]
u'	dimensionless velocity of bulk liquid, $u/[\sigma g(\rho_l-\rho_v)/\rho_v^2]^{1/4}$
V	instantaneous volume of bubble [m^3]
v_l	volumetric growth rate of bubble [m^3 s^{-1}]

Greek symbols

δ_c	critical thickness of liquid film [m]
λ'_D	most susceptible (or dangerous) Taylor wavelength [m]
ρ_l	density of liquid [kg m^{-3}]
ρ_v	density of vapor [kg.m^{-3}]
σ	surface tension [N m^{-1}]
τ_d	hovering period of bubble [s]

1. INTRODUCTION

WHEN high heat flux nucleate boiling takes place on a uniformly heated horizontal cylinder in an upward cross flow of saturated liquid, vapor removal from the cylinder takes place with two different flow patterns according to the bulk liquid velocity. If the liquid velocity is very low, a flow pattern such as illustrated in Fig. 1 appears, where the vapor generated at the cylinder wall accumulates in a massive vapor bubble at approximately equal intervals, and each bubble separates away from the cylinder when it has grown sufficiently. On the other hand, if the liquid velocity is sufficiently high, a 2-dim. 'sheet-like' escape flow of vapor appears instead of the 3-dim. 'bubble-like' flow. These two types of escape flow patterns were found by Cochran and Andracchio [1] by means of high-speed photography, and later, Lienhard and Eichhorn [2] presented a criterion for the transition between the two flow patterns. In addition, McKee and Bell [3] showed by experiment that when the diameter of the cylinder is increased beyond a certain value under the condition of fixed bulk liquid velocity, a rapid reduction of CHF takes place. This phenomenon may also result from the change of vapor escape flow pattern.

In the paper by Cochran and Andracchio [1], semi-empirical analyses of CHF were presented for the cases

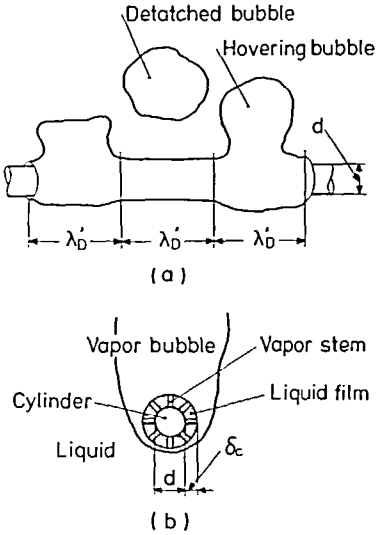

FIG. 1. Nucleate boiling on a horizontal cylinder with bubble-like escape flow of vapor at high heat fluxes.

of the bubble-like and the sheet-like escape flows. In the former case, the effect of forced convection heat transfer was added to the Lienhard prediction of pool boiling CHF, while in the latter, the Vliet–Leppert prediction equation of CHF was employed based on the concept that CHF is connected to the dryout of the heated surface at the rear stagnation point of the cylinder. This means that different models were assumed to predict CHF for the two types of escape flow pattern.

Recently, however, the present authors [4] have presented a new hydrodynamic model of CHF, predicting the CHF on a uniformly heated horizontal cylinder, not only in 'pool boiling' with a bubble-like escape flow, but also in 'forced convection boiling' with a sheet-like escape flow. In the present paper, therefore, the analysis of CHF in pool boiling is extended to the case of the forced cross flow at low velocities accompanied by bubble-like escape flow, and the results obtained are compared with the existing data including the transition from the bubble-like to the sheet-like escape flow region.

2. THEORETICAL ANALYSIS

2.1. *CHF with bubble-like escape flow of vapor*

Figure 1 is a reproduction of a figure shown in a previous paper [4], illustrating the flow configuration around an infinitely long, horizontal cylinder in the bubble-like escape flow region. In Fig. 1(a), λ'_D represents the most susceptible (or dangerous) wavelength of Taylor instability, which has been given by Lienhard and Wong [5] for a horizontal, cylindrical vapor–liquid interface in a stationary bulk liquid as

$$\lambda'_D = (\sqrt{3})2\pi\left[\frac{\sigma}{g(\rho_l-\rho_v)}\right]^{1/2}\left[1+\frac{2\sigma}{d^2g(\rho_l-\rho_v)}\right]^{-1/2}. \quad (1)$$

When the cylindrical interface is subject to a forced cross flow of bulk liquid, equation (1) must be modified. However, the bubble-like escape flow of vapor takes place at very low bulk liquid velocities, to which equation (1) may possibly apply approximately without serious error.

Figure 1(b) illustrates the situation of a liquid film wetting the cylinder surface surrounded by a massive vapor bubble. This liquid film has numerous, columnar vapor stems of the bubble in it when the film is sufficiently thick, so the heat transferred from the cylindrical wall is absorbed by latent heat at the part of the vapor–liquid interface of vapor stems near the heated surface, and the vapor thus generated flows through the vapor stems to enter the surrounding massive vapor bubble. When the thickness of the liquid film reduces considerably, evaporation takes place at the outer surface of the liquid film as well. In any case, however, the heat flux q is related to the volumetric growth rate v_1 of a surrounding vapor bubble via the heat balance as follows:

$$v_1 = \pi d\lambda'_D q/(\rho_v H_{fg}). \quad (2)$$

The vapor bubble, thus nourished with vapor from the underlying liquid film, separates from the cylinder when it has grown sufficiently. After a bubble leaves the cylinder, a new one is immediately established in its place. This periodic bubble formation can be assumed to take place with a mean period τ_d. Now, if the liquid film blanketed by a vapor bubble is fed with liquid from the bulk region only when the bubble separates from the cylinder (see ref. [4] for details), then it can be postulated that CHF appears when the liquid film evaporates out at the end of the hovering period τ_d, for which the heat balance is written as

$$\tau_d q A_w = \rho_l \delta_c (A_w - A_v + A_w\delta_c/d)H_{fg} \quad (3)$$

where δ_c is the initial thickness of the liquid film [see Fig. 1(b)], A_w the area of the heated surface, and A_v the cross-sectional area of the vapor stems.

The three unknowns δ_c, A_v/A_w, and τ_d included in equation (3) are evaluated as follows. First, the initial thickness of the liquid film δ_c, which is the critical thickness of a liquid film capable of stabilizing itself on a solid wall, has been determined in the authors' previous paper [4] on the basis of the Helmholtz instability of the vapor–liquid interface of vapor stems as

$$\delta_c = \frac{\pi}{2}\sigma\frac{\rho_l+\rho_v}{\rho_l\rho_v}\left(\frac{A_v}{A_w}\right)^2\left(\frac{\rho_v H_{fg}}{q}\right)^2 \quad (4)$$

where A_v/A_w is given as a very weak function of ρ_v/ρ_l by

$$A_v/A_w = 0.0584(\rho_v/\rho_l)^{0.2}. \quad (5)$$

Finally, the hovering period of the bubble τ_d is determined through the following theoretical analysis of the bubble behavior by means of such an idealized model as illustrated in Fig. 2 [6], where a spherical bubble, being nourished with vapor from a fixed point P, is moving upward due to the buoyant force. For this bubble, the equation of motion is written as

$$\frac{d}{dt}\left[\left(\frac{11}{16}\rho_l+\rho_v\right)V\left(\frac{ds}{dt}-u\right)\right] = (\rho_l-\rho_v)Vg \quad (6)$$

where 11/16 is the theoretical volumetric ratio of the accompanying liquid to a moving spherical bubble [6], V the bubble volume at the time t after the commencement of bubble growth, s the height of the bubble center O measured from the fixed point P, and u the vertical upward velocity of bulk liquid. (Note that

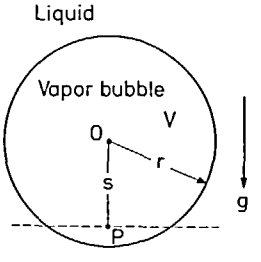

FIG. 2. A model of vapor bubble growing through the feed of vapor as well as rising due to the buoyancy.

$ds/dt - u$ is the relative velocity of the bubble center to the bulk liquid.)

In equation (6), V is evaluated by

$$V = v_1 t \tag{7}$$

where v_1 is the volumetric growth rate of the bubble given by equation (2). It is noted in Fig. 2 that although the bubble center O rises continuously after $t = 0$, the state of $s < r$ {where $r = [3V/(4\pi)]^{1/3}$} can hold for a certain period due to the increase of the bubble volume V, which determines the hovering period of the bubble τ_d. Thus, solving equation (6) together with equation (7) for $s(t)$, and taking into account the initial condition $s = 0$ at $t = 0$ as well as the departure condition $s = r = [3V/(4\pi)]^{1/3}$ at $t = \tau_d$, yields

$$\tau_d = \left(\frac{3}{4\pi}\right)^{1/5}\left[\frac{4(\xi\rho_l+\rho_v)}{g(\rho_l-\rho_v)}\right]^{3/5} \times v_l^{1/5}\left[1+\frac{4(\xi\rho_l+\rho_v)u}{\tau_d g(\rho_l-\rho_v)}\right]^{3/5} \tag{8}$$

where $\xi = 11/16$.

Now, ignoring A_v/A_w as compared with unity in equation (3), since $A_v/A_w < 0.0584$ as is noted in equation (5), and solving equations (1)–(5) and (8) for the critical heat flux q, and finally writing the q as q_{c0} results in

$$\frac{q_{c0}}{q_{c0,Z}} = \left(\frac{\sqrt{3}}{R'}\right)^{1/16}\left[1+\frac{1}{2(R')^2}\right]^{1/32} \times \left[1+0.156\left(\frac{\rho_v}{\rho_l}\right)^{0.4}\left(1+\frac{\rho_v}{\rho_l}\right)\frac{1}{R'}\frac{1}{(q_{c0}/q_{c0,Z})^2}\right]^{5/16} \times \left[\frac{1+1.68\dfrac{\frac{11}{16}+\frac{\rho_v}{\rho_l}}{\left(\frac{\rho_v}{\rho_l}\right)^{0.4}\left(1+\frac{\rho_v}{\rho_l}\right)}\times\dfrac{\left(\frac{q_{c0}}{q_{c0,Z}}\right)^3}{1+0.156\left(\frac{\rho_v}{\rho_l}\right)^{0.4}\left(1+\frac{\rho_v}{\rho_l}\right)\frac{1}{R'}\frac{1}{(q_{c0}/q_{c0,Z})^2}}u'}\right]^{1/16} \tag{9}$$

where

$$R' = (d/2)/[\sigma/g(\rho_l-\rho_v)]^{1/2},$$

$$u' = u/[\sigma g(\rho_l-\rho_v)/\rho_v^2]^{1/4},$$

and $q_{c0,Z}$ is the critical heat flux in pool boiling on an infinite, upward-facing, horizontal flat plate [4], which can be derived from the foregoing analysis with three necessary modifications for an infinite plate: $d \to \infty$ in equations (1) and (3), $v_1 = (\lambda_D')^2 q/(\rho_v H_{fg})$ in place of equation (2), and $u = 0$ in equation (8). When the numerical value of $q_{c0,Z}$ in equation (9) is required, it is calculated by the following Zuber equation. (See Section 2.3 in ref. [4] for details.)

$$\frac{q_{c0,Z}}{\rho_v H_{fg}}\Big/\left[\frac{\sigma g(\rho_l-\rho_v)}{\rho_v^2}\right]^{1/4} = 0.131. \tag{10}$$

Table 1. Values of $q_{c0}/q_{c0,Z}$ predicted by equation (9)

u'	ρ_v/ρ_l	R' 0.1	0.2	0.5	1.0	5.0	10
0	0.0001	1.360	1.246	1.120	1.049	0.936	0.896
	0.001	1.373	1.253	1.123	1.051	0.937	0.896
	0.01	1.402	1.270	1.131	1.055	0.938	0.897
	0.1	1.472	1.313	1.153	1.067	0.940	0.898
	1	1.699	1.470	1.243	1.123	0.956	0.906
0.01	0.0001	1.433	1.301	1.158	1.079	0.956	0.913
	0.001	1.406	1.277	1.140	1.064	0.945	0.903
	0.01	1.416	1.280	1.138	1.060	0.941	0.900
	0.1	1.477	1.317	1.156	1.069	0.942	0.899
	1	1.701	1.472	1.244	1.124	0.956	0.907
0.1	0.0001	1.642	1.478	1.301	1.203	1.051	0.998
	0.001	1.553	1.397	1.231	1.139	0.999	0.951
	0.01	1.502	1.347	1.187	1.099	0.968	0.922
	0.1	1.521	1.350	1.178	1.087	0.954	0.910
	1	1.723	1.488	1.255	1.132	0.962	0.912
1	0.0001	1.951	1.755	1.543	1.424	1.239	1.174
	0.001	1.829	1.642	1.441	1.329	1.157	1.096
	0.01	1.734	1.549	1.354	1.247	1.084	1.028
	0.1	1.694	1.496	1.295	1.187	1.029	0.976
	1	1.845	1.585	1.328	1.193	1.006	0.951

The root $q_{c0}/q_{c0,Z}$ of equation (9) can be solved by computer as a function of R', ρ_v/ρ_l and u'. Some of the results thus obtained are listed in Table 1, where the values of $q_{c0}/q_{c0,Z}$ in the case of $u' = 0$ are found to agree with those obtained in the previous paper [4] for saturated pool boiling on a horizontal cylinder. In Fig. 3, the prediction of equation (9) in the case of $u' = 0$ is compared satisfactorily with the range of about 900 experimental data points of CHF in pool boiling collected by Sun and Lienhard [7].

2.2. *CHF with sheet-like escape flow of vapor*

Figure 4 illustrates the flow structures at high bulk liquid velocities accompanied by a sheet-like escape flow of vapor. In this case, if the bulk liquid velocity is sufficiently high, q_{c0} is hardly affected by gravity, and the analysis of q_{c0} presented in the present authors' previous paper [4] is summarized as follows. A liquid film flowing over a cylinder wall receives saturated liquid constantly at the front stagnation point with δ_c in

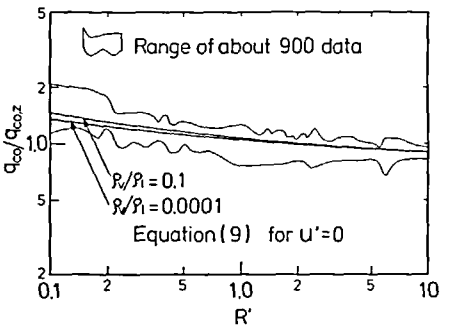

FIG. 3. Critical heat flux in saturated pool boiling for horizontal cylinders.

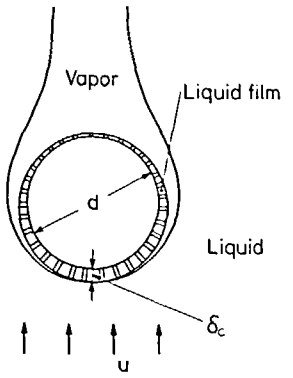

FIG. 4. Nucleate boiling on a cylinder in a cross flow with a sheet-like escape flow of vapor at high heat fluxes.

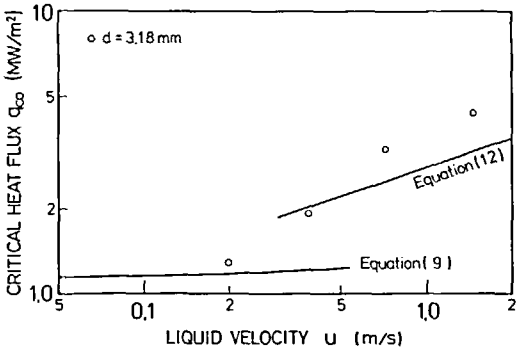

FIG. 6. Variation of q_{c0} with u for water at atmospheric pressure ($\rho_v/\rho_l = 0.000624$).

film thickness from the bulk flow of velocity u, which causes CHF when the liquid film flow drys up at the rear stagnation point, and the heat balance is written as

$$q\pi d/2 = \rho_l \delta_c u H_{fg}. \tag{11}$$

Solving equations (4), (5) and (11) for the critical heat flux q, and writing the q as q_{c0} results in

$$\frac{q_{c0}}{GH_{fg}} = 0.151\left(\frac{\rho_v}{\rho_l}\right)^{0.467}\left(1+\frac{\rho_v}{\rho_l}\right)^{1/3}\left(\frac{\sigma\rho_l}{G^2 d}\right)^{1/3} \tag{12}$$

where $G = u\rho_l$, that is, the mass velocity of the bulk liquid flow. Except for the case of $\rho_v/\rho_l > 0.1$, $(1+\rho_v/\rho_l)^{1/3}$ on the RHS of equation (12) may be approximated as unity.

3. COMPARISON WITH EXPERIMENTAL DATA

3.1. *Change of CHF with bulk liquid velocity*

Figure 5 shows a comparison of q_{c0} predicted by equations (9) and (12) with the experimental data obtained by Cochran and Andracchio [1] for saturated water at atmospheric pressure ($\rho_v/\rho_l = 0.000624$). Bubble and sheet regions indicated by directed lines in Fig. 5 are the results observed in ref. [1] by means of high-speed photography.

Figure 6 shows a similar comparison for saturated water at atmospheric pressure ($\rho_v/\rho_l = 0.000624$), though the diameter of the cylinder is somewhat greater than that in Fig. 5. Experimental data are those obtained by the extrapolation of the subcooling temperature $\Delta t_{sub} \to 0$ in Fig. 4 of Vliet and Leppert's paper [8].

Figure 7 shows a comparison for saturated R-113 at near atmospheric pressure ($\rho_v/\rho_l = 0.00645$), and experimental data are those obtained by Cochran and Andracchio [1]. According to ref. [1], the vapor removal processes in the present case resemble a bubble-like phenomenon for all the data points in Fig. 7, with no evidence of a long sheet of vapor being torn away from the vapor cavity behind the cylinder.

Figure 8 refers to the data obtained by Yilmaz and Westwater [9] for pool boiling as well as for forced convection boiling of saturated R-113 at near atmospheric pressure ($\rho_v/\rho_l = 0.00489$) on a cylinder of considerably large diameter.

Figure 9 refers to the data of R-12 at 7.85 bar ($\rho_v/\rho_l = 0.035$) measured by Cumo *et al.* [10] with very low velocities and a large cylinder diameter. Although the data points plotted in Fig. 9 are somewhat special ones obtained by heating the central tube alone in a horizontal tube bundle of staggered arrangement, the liquid velocity crossing the tube bundle is so low that the condition of the CHF on a single cylinder may be approximated.

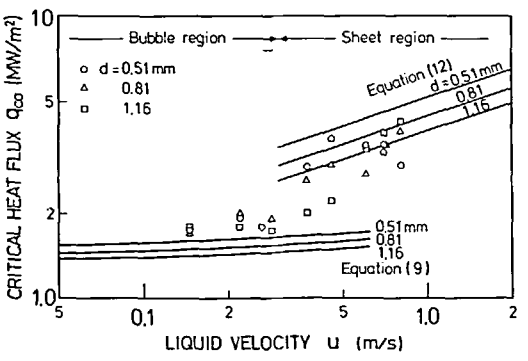

FIG. 5. Variation of q_{c0} with u for water at atmospheric pressure ($\rho_v/\rho_l = 0.000624$).

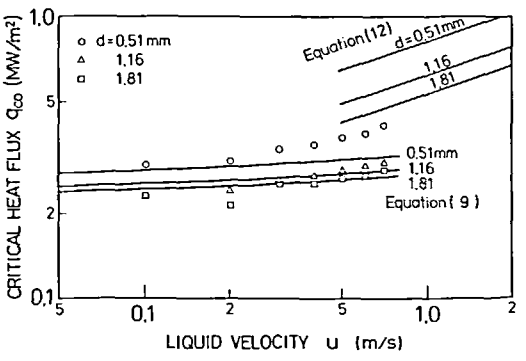

FIG. 7. Variation of q_{c0} with u for R-113 at 1.34 bar ($\rho_v/\rho_l = 0.00645$).

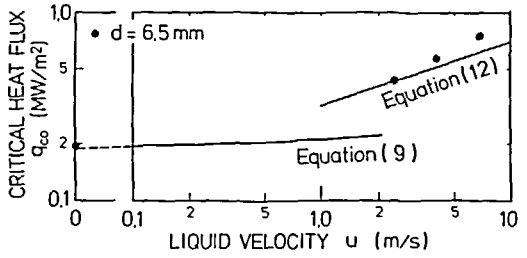

FIG. 8. Variation of q_{c0} with u for R-113 at near atmospheric pressure ($\rho_v/\rho_l = 0.00489$).

Finally, Fig. 10 shows a comparison of the predictions of equations (9) and (12) with the CHF data of isopropanol at near atmospheric pressure ($\rho_v/\rho_l = 0.00299$) measured by Hasan *et al.* [11].

3.2. *Change of CHF with diameter of cylinder*

Figure 11 shows the change of critical heat flux q_{c0} with the diameter of the cylinder under fixed condition of bulk liquid velocity for saturated water at atmospheric pressure ($\rho_v/\rho_l = 0.000624$). In Fig. 11, circular symbols refer to the data obtained by McKee and Bell [3], while triangular symbols refer to the data of Vliet and Leppert [12].

4. DISCUSSION

(1) Although comparisons between the prediction and the data are rather limited in number, the results of Figs. 5–11 show that the prediction of equation (9) for the CHF in the bubble-like escape flow region is fairly successful except for Fig. 10, where the data for $d = 0.50$ and 0.81 mm appear too high as compared with the data for $d = 1.50$ mm.

(2) As for the prediction of equation (12) for the CHF in the sheet-like escape flow region, it has been shown in the present authors' previous paper [4] that there are a few secondary problems to be solved if much better agreement with the experimental data is required. However, as far as the rough trend in the change of CHF is concerned, the prediction of equation (12) seems to agree with the data within the range of conditions dealt with in this paper.

Postulating 'mechanical energy stability criterion', Lienhard and Eichhorn [2] formerly presented a semi-

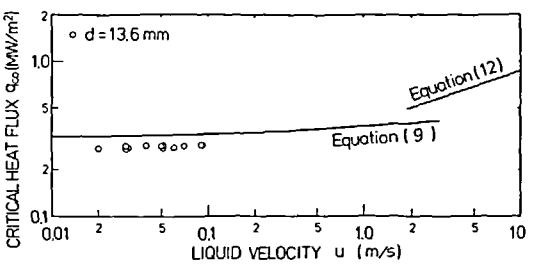

FIG. 9. Variation of q_{c0} with u for R-12 at 7.85 bar ($\rho_v/\rho_l = 0.035$).

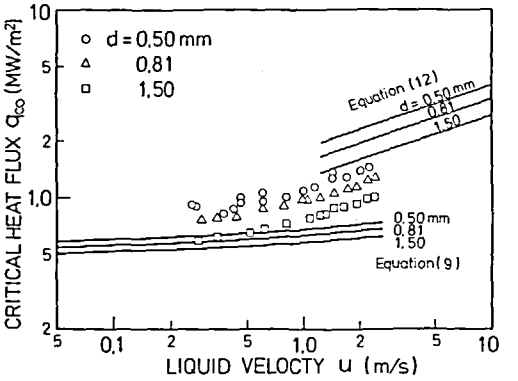

FIG. 10. Variation of q_{c0} with u for isopropanol at near atmospheric pressure ($\rho_v/\rho_l = 0.00299$).

theoretical generalized correlation for the CHF in the sheet-like escape flow region, which was composed of a prediction of q_{c0} in the low-velocity region,

$$\frac{\pi q_{c0}}{\rho_v H_{fg} u} = 1 + 4^{1/3}\left(\frac{\sigma}{\rho_v u^2 d}\right)^{1/3}, \tag{13}$$

a prediction of q_{c0} in the high-velocity region,

$$\frac{\pi q_{c0}}{\rho_v H_{fg} u} = \frac{1}{169}\left(\frac{\rho_l}{\rho_v}\right)^{3/4} + \frac{1}{19.2}\left(\frac{\rho_l}{\rho_v}\right)^{1/2}\left(\frac{\sigma}{\rho_v u^2 d}\right)^{1/3} \tag{14}$$

and a prediction of q_{c0} in the transition region between the foregoing two regions,

$$\frac{\pi q_{c0}}{\rho_v H_{fg} u} = 0.275\left(\frac{\rho_l}{\rho_v}\right)^{1/2} + 1. \tag{15}$$

This correlation suffers from a rather strange trend in the range of $\rho_v/\rho_l > 0.00108$, where q_{c0} predicted by equation (13) is always higher than that of equation (14).

Recently, taking into account such the data as plotted in the sufficiently high velocity regions of Figs. 6, 8 and 10, Hasan *et al.* [11] modified equation (14) as follows:

$$\frac{\pi q_{c0}}{\rho_v H_{fg} u} = \frac{1}{1090}\left(\frac{\rho_l}{\rho_v}\right) + \frac{1}{66.6}\left(\frac{\rho_l}{\rho_v}\right)^{2/3}\left(\frac{\sigma}{\rho_v u^2 d}\right)^{1/3} \tag{14a}$$

to predict only the CHF unaffected by gravity. If G is employed instead of u, equation (14a) can be rewritten

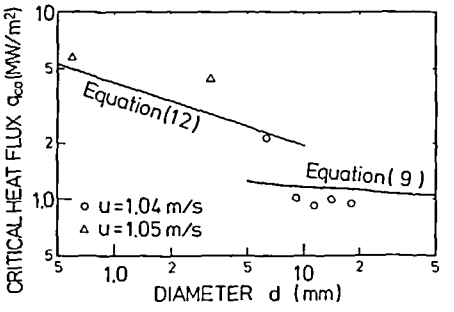

FIG. 11. Variation of q_{c0} with d for water at atmospheric pressure ($\rho_v/\rho_l = 0.000624$).

as

$$\frac{q_{c0}}{GH_{fg}} \simeq 0.000292 + 0.00478\left(\frac{\sigma\rho_l}{G^2 d}\right)^{1/3}. \quad (14b)$$

When both ρ_v/ρ_l and $\sigma\rho_l/G^2 d$ are moderate in magnitude, q_{c0}'s predicted by equations (12) and (14b) are close to each other, but when either ρ_v/ρ_l is extremely high or when $\sigma\rho_v/G^2 d$ is extremely low, the predictions of the two equations depart from each other.

(3) For the transition from the bubble-like flow region toward the sheet-like flow region, Lienhard and Eichhorn [2] gave the following tentative criterion:

$$\rho_v u^2 d/\sigma = 4(\rho_l/\rho_v)R' \quad (16)$$

while Yilmaz and Westwater [9] referred to another criterion of Lienhard and Eichhorn,

$$\rho_v u^2 d/\sigma = 0.1(\rho_v/\rho_l)(R')^2. \quad (17)$$

When compared with the results of Figs. 5–10, equation (16) appears to be unsuitable, while equation (17) is regarded as tolerable, but the latter equation still seems to underpredict the critical velocity and overpredict the critical diameter. According to the analysis developed in the present study, equation (17) may probably be improved by taking into account not only $\rho_v u^2 d/\sigma$, ρ_v/ρ_l and R' but also u'.

Recently Hasan *et al.* [11] presented a critical value,

$$u'/(\rho_v/\rho_l)^{1/2} = 10, \quad (18)$$

above which gravity is assumed to exert no influence on q_{c0}, corresponding to the applicable range of equation (14a). It seems likely that equation (18) is different in character from the criterion of equation (17), being unable to explain, for example, the phenomenon of the critical diameter shown in Fig. 11.

5. CONCLUSIONS

(1) CHF on a horizontal cylinder in an upward cross flow has been analyzed on the basis of a new hydrodynamic instability model proposed in the present authors' previous paper [4]. The predictions thus obtained are compared satisfactorily with the existing experimental data, mainly for the CHF in the bubble-like flow region and for the trend of the transition from the bubble-like to the sheet-like escape flow region.

(2) Experiments of the CHF on a horizontal cylinder in an upward cross flow at comparatively low velocities are extremely limited in the extent of the experimental conditions as well as in the number of data. Accordingly, further experimental studies are needed to establish a more reliable and comprehensive knowledge of this phenomenon.

Acknowledgements—The support for this work provided by the Ministry of Education, Science and Culture: Special Project Research on Energy Grant No. 57040016 (1982) is gratefully acknowledged.

REFERENCES

1. T. H. Cochran and C. R. Andracchio, Forced-convection peak heat flux on cylindrical heaters in water and refrigerant 113, NASA D-7553 (1974).
2. J. H. Lienhard and R. Eichhorn, Peak boiling heat flux on cylinders in a cross flow, *Int. J. Heat Mass Transfer* **19**, 1135–1142 (1976).
3. H. R. McKee and K. J. Bell, Forced convection boiling from a cylinder normal to the flow, *A.I.Ch.E. Symp. Ser.* 65(92), 222–230 (1969).
4. Y. Haramura and Y. Katto, A new hydrodynamic model of critical heat flux, applicable widely to both pool and forced convection boiling on submerged bodies in saturated liquid, *Int. J. Heat Mass Transfer* **26**, 389–399 (1983).
5. J. H. Lienhard and P. T. Y. Wong, The dominant unstable wavelength and minimum heat flux during film boiling on a horizontal cylinder, *Trans. Am. Soc. Mech. Engrs*, Series C, *J. Heat Transfer* **86**, 220–226 (1964).
6. Y. Katto and S. Yokoya, Behavior of a vapor mass in saturated nucleate and transition pool boiling, *Heat Transfer—Japan. Res.* 5(2), 45–65 (1976).
7. K. H. Sun and J. H. Lienhard, The peak pool boiling heat flux on horizontal cylinders, *Int. J. Heat Mass Transfer* **13**, 1425–1439 (1970).
8. G. C. Vliet and G. Leppert, Critical heat flux for subcooled water flowing normal to a cylinder, *Trans. Am. Soc. Mech. Engrs*, Series C, *J. Heat Transfer* **86**, 68–74 (1964).
9. S. Yilmaz and J. W. Westwater, Effect of velocity on heat transfer to boiling Freon-113, *Trans. Am. Soc. Mech. Engrs*, Series C, *J. Heat Transfer* **102**, 26–31 (1980).
10. M. Cumo, G. E. Farello, J. Gasiorowski, G. Iovino and A. Naviglio, Quality influence on DNB in cross flows through bundles, CNEN-RT/ING(78)10 (1978).
11. M. Z. Hasan, M. M. Hasan, R. Eichhorn and J. H. Lienhard, Boiling burnout during crossflow over cylinders, beyond the influence of gravity, *Trans. Am. Soc. Mech. Engrs*, Series C, *J. Heat Transfer* **103**, 478–484 (1981).
12. G. C. Vliet and G. Leppert, Critical heat flux for nearly saturated water flowing normal to a cylinder, *Trans. Am. Soc. Mech. Engrs*, Series C, *J. Heat Transfer* **86**, 59–67 (1964).

FLUX THERMIQUE CRITIQUE POUR UN CYLINDRE HORIZONTAL UNIFORMEMENT CHAUFFE DANS UN ECOULEMENT TRANSVERSAL ASCENDANT DE LIQUIDE SATURE

Résumé—On rapporte les résultats d'une étude analytique du flux thermique critique (CHF) sur un cylindre horizontal chauffé uniformément dans un écoulement transversal ascendant de liquide saturant. Deux sortes d'écoulement de sortie de vapeur sont considérées: l'une est l'écoulement de bulles dans le domaine des très faibles vitesses et l'autre est l'écoulement comme feuilleté dans le domaine des vitesses suffisamment élevées. Un nouveau modèle d'instabilité hydrodynamique de CHF proposé récemment par les auteurs est employé dans cette analyse et on montre que la prédiction de CHF est bonne, comparée aux données existantes.

KRITISCHE WÄRMESTROMDICHTE AN EINEM GLEICHFÖRMIG BEHEIZTEN HORIZONTALEN ZYLINDER IN DER AUFWÄRTSGERICHTETEN QUERSTRÖMUNG EINER GESÄTTIGTEN FLÜSSIGKEIT

Zusammenfassung—Diese Arbeit berichtet über die Ergebnisse einer analytischen Untersuchung der kritischen Wärmestromdichte (CHF) an einem gleichförmig beheizten horizontalen Zylinder in einer aufwärtsgerichteten Querströmung einer gesättigten Flüssigkeit. Es werden zwei Strömungsformen des entweichenden Dampfes betrachtet: blasenähnliche Strömung im Bereich sehr kleiner Geschwindigkeiten und streifenförmige Strömung im Bereich genügend hoher Geschwindigkeiten. Ein neues hydrodynamisches Instabilitätsmodell für die kritische Wärmestromdichte, das kürzlich von den Autoren vorgeschlagen wurde, wird heier verwendet. Es zeigt sich, daß die Vorhersage der kritischen Wärmestromdichte recht gut mit den bestehenden Daten übereinstimmt.

КРИТИЧЕСКИЙ ТЕПЛОВОЙ ПОТОК НА РАВНОМЕРНО НАГРЕТОМ ГОРИЗОНТАЛЬНОМ ЦИЛИНДРЕ ПРИ ПОПЕРЕЧНОМ ОБТЕКАНИИ ВОСХОДЯЩИМ ТЕЧЕНИЕМ НАСЫЩЕННОЙ ЖИДКОСТИ

Аннотация—Представлены результаты аналитического исследования критического теплового потока (КТП) на равномерно нагретом горизонтальном цилиндре при поперечном обтекании восходящим течением жидкости, находящейся на линии насыщения. Учтены два типа течения образующегося пара: одно в виде пузырьков в диапазоне очень малых скоростей и второе—слоистое в диапазоне достаточно высоких скоростей. Для анализа используется недавно предложенная авторами новая модель гидродинамической неустойчивости при КТП. Показано, что рассчитанные значения КТП довольно хорошо согласуются с имеющимися экспериментальными данными.